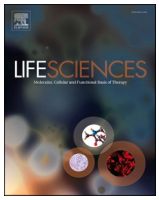
Life Sciences 306 (2022) 120781



Contents lists available at ScienceDirect

Life Sciences

journal homepage: www.elsevier.com/locate/lifescie





7,8-Dihydroxyflavone alleviates Endoplasmic Reticulum Stress in cafeteria diet-induced metabolic syndrome

Elif Sahin [a,*], Neslihan Saglam [a], Seniz Erdem [a], Elif Alvuroglu [b], Ismail Abidin [c], Esin Yulug [b], Ahmet Alver [d]

[a] Department of Medical Biochemistry, Graduate School of Medical Science, Karadeniz Technical University, Trabzon, Turkiye
[b] Department of Histology and Embryology, Faculty of Medicine, Karadeniz Technical University, Trabzon, Turkiye
[c] Department of Biophysics, Faculty of Medicine, Karadeniz Technical University, Trabzon, Turkiye
[d] Department of Medical Biochemistry, Faculty of Medicine, Karadeniz Technical University, Trabzon, Turkiye

ARTICLE INFO

Keywords:
Insulin resistance
Liver
Pancreas
Inflammation
BDNF

ABSTRACT

Aims: Prolonged Endoplasmic Reticulum Stress (ERS) is involved in the pathogenesis of metabolic syndrome, including type-2 diabetes mellitus, cardiovascular diseases, atherosclerosis, obesity, and fatty liver disease. There have been significant efforts to discover molecules to treat ERS and/or to ameliorate associate symptoms. In this study, we investigated the effect of 7,8-Dihydroxyflavone (7,8-DHF) on ERS in liver and pancreas tissues in a cafeteria (CAF) diet induced metabolic syndrome model.

Main methods: Male C57BL/6 mice were fed CAF diet for 16 weeks and 7,8-DHF was administered intraperitoneally (5 mg/kg/day) for last four weeks. 78-kDa glucose-regulated protein (GRP78) and C/EBP homologous protein (CHOP) in liver and pancreas tissues, insulin and interleukin-1β (IL-1β) in serum were analyzed by ELISA method and serum biochemistry parameters were analyzed with autoanalyzer. GRP78 and CHOP gene expression levels were determined by qRT-PCR. In addition, histopathological analyzes were performed on liver and pancreas tissues.

Key findings: Findings revealed that CAF diet caused metabolic abnormalities, insulin resistance and inflammation in serum and triggered ERS in pancreas and liver tissues. 7,8-DHF treatment significantly reduced metabolic abnormalities by reducing serum biochemical parameters, HOMO-IR and IL-1β levels. qRT-PCR and ELISA results indicated that 7,8-DHF treatment down-regulated GRP78 and CHOP expression and protein levels in the liver and GRP78 expression in pancreas. Efficiency of 7,8-DHF in these tissues was also demonstrated by histopathological tests.

Significance: In conclusion, CAF diet-induced metabolic syndrome model, 7,8-DHF suppressed ERS and ERS-induced metabolic disorders in both liver and pancreas. Therefore, 7,8-DHF may potentially be a novel therapeutic compound to ameliorate ERS and related metabolic symptoms.

1. Introduction

Metabolic syndrome, also known as “syndrome X”, “insulin resistance” or “deadly quartet” by WHO, refers to a pathological state characterized by conditions such as abdominal obesity, insulin resistance, hypertension and hyperlipidemia, and has now become a global epidemic. For this reason, it is a combination of diseases such as cardiovascular diseases, obesity and diabetes, rather than a single disease [1]. This complex pathological condition is usually caused by high caloric intake and low energy consumption. In addition, genetic

Abbreviations: ERS, Endoplasmic Reticulum Stress; 7,8-DHF, 7,8-dihydroxyflavone; CAF, cafeteria; GRP78, 78-kDa glucose-regulated protein; CHOP, C/EBP homologous protein; ER, endoplasmic reticulum; UPR, unfolded protein response; BDNF, Brain Derived Neurotrophic Factor (BDNF); TrkB, tropomyosin-related kinase receptor type B; DMSO, dimethyl sulfoxide; EAT, epididymal adipose tissue; ALT, alanine aminotransferase; HOMA-IR, Homeostatic Model Assessment of Insulin Resistance; OGTT, Oral Glucose Tolerance Test; TUNEL, deoxynucleotidyl transferase (TdT) deoxyuridine triphospate nick end labeling; DAB, 3,3′-diaminobenzidine; AI, apoptotic indexes; PI3K, phosphoinositide 3-kinases; Ras-MAPK, Ras-mitogen-activated protein kinase; PKC, phospholipase C1 (PLC-1)-protein kinase C.

* Corresponding author.
E-mail address: elifsahin@ktu.edu.tr (E. Sahin).

https://doi.org/10.1016/j.lfs.2022.120781
Received 17 June 2022; Received in revised form 29 June 2022; Accepted 1 July 2022
Available online 11 July 2022
0024-3205/© 2022 Elsevier Inc. All rights reserved.

predispositions, sedentary lifestyle, and even the composition of the individual's intestinal microbiota also contribute to the development of metabolic syndrome [2].

The endoplasmic reticulum (ER) is a highly dynamic and important organelle found in all eukaryotic cells. Most of the structural and secretory proteins become functional by undergoing post-translational modification, folding, and oligomerization in the ER lumen. Therefore, maintenance of ER homeostasis and function is vital for normal cellular function. Increased levels of unfolded/misfolded proteins within the ER lumen lead to a condition commonly referred to as 'ERS'. To combat ERS, cells have developed an adaptive stress response called the unfolded protein response (UPR). Misfolded and/or unfolded proteins are directed to the ER-associated degradation system, which is a component of the UPR, followed by proteasomal degradation. If the UPR fails, the cell is directed to apoptosis [3]. Glucose-regulated protein 78 (GRP78) belongs to the family of heat shock proteins. It is an ER luminal protein whose expression is induced during ER stress and plays a recently identified protective role in preventing ER stress-induced cell death. As an ER chaperone, GRP78 modulates the UPR signaling network. Under ER stress conditions, it dissociates from PERK, a branch of the UPR, and binds to unfolded or misfolded proteins. C/EBP homologous protein (CHOP) is another major player responsible for apoptotic cell death induced by ER stress. CHOP is mainly found in the cytoplasm and under normal conditions its expression level is very low. When ER stress is induced, CHOP expression is significantly increased, activated and transported to the nucleus. Overexpression of CHOP promotes cell cycle arrest or apoptosis [3,4]. During ER stress, many pathways are disrupted in essential metabolic tissues associated with energy metabolism, such as the adipose tissue, liver and pancreas. ER stress causes hepatic steatosis by regulating inflammation and lipid synthesis in the liver. Similarly, hepatic steatosis triggers ER stress. In pancreatic beta cells, it impairs glucose-stimulated insulin secretion. Although the exact mechanism has not been elucidated, ERS has been shown to play a role in the pathogenesis of metabolic diseases such as obesity, atherosclerosis, diabetes, myocardial dysfunction and non-alcoholic fatty liver disease. Therefore, for the treatment of such diseases, the development of novel treatment strategies that suppress ERS has most importance [5].

7,8-dihydroxyflavone (7,8-DHF) is a monomeric compound belonging to the flavone family that occurs naturally in the leaves of *Godmania aesculifolia*, *Tridax procumbens* and *primula* tree. It has been identified as a functional Brain Derived Neurotrophic Factor (BDNF) mimetic and its receptor tropomyosin-related kinase receptor type B (TrkB) agonist. 7,8-DHF imitates BDNF and acts as a robust TrkB agonist [6]. BDNF is known to be effective in food intake regulation and body weight control, as well as its main effect on the nervous system [7]. BDNF has been shown to improve glucose and lipid metabolism and control energy homeostasis in obese diabetic mice [8]. BDNF's short half-life and inability to cross the blood-brain barrier cause problems in its clinical application [9]. On the other hand, 7,8-DHF has a longer half-life than BDNF, and it can imitate the effects of BDNF by binding its TrkB receptor by crossing the blood-brain barrier significantly [10]. It has been shown that 7,8-DHF has an anti-obesity effect [11–13] and can protect cells from oxidative stress in some cell culture studies [14–17]. Although 7,8-DHF has been shown to protect cells against some cytotoxic agents and oxidative damage in cell culture studies, *in vivo* studies against ERS are limited.

In this study, we aimed to examine the effect of 7,8-DHF on ERS in liver and pancreas tissues which are essential tissues for energy metabolism in a cafeteria diet-induced experimental metabolic syndrome model. In this context, the effect of 7,8-DHF on insulin resistance and general metabolic status were investigated. The findings showed that 7,8-DHF reduced ERS in liver and pancreas tissues, suppressed glucose intolerance and insulin resistance.

2. Material and methods

2.1. Animals and procedure

This study was approved by Karadeniz Technical University Animal Experiments Local Ethics Committee with protocol number 2019/37 dated 05.09.2019. C57BL/6 mice used in the experiment were obtained from Karadeniz Technical University Faculty of Medicine, Surgical Research Center, where they are housed and bred. 5–6 week old male mice weighing 17–20 g were used for the experiment. Animals were housed and fed individually in ventilated mouse cages (RAIR IsoSystem, Seaford, DE USA). A 12-hour dark-light environment was provided in the room. The proteins measured in this study, have been previously measured in several previous studies done in our lab. Using this data, the effect size was calculated with the G*Power program. With the entered effect size (0.60), alpha error (0.05), power (0.85) and group number (4) values, the total sample size is found 40. Calculated as 10 animals per group. Food and water were given *ad libitum*. Four experimental groups were formed and each group consisted of 10 mice.

Control group (C): They were fed with rodent diet (Bayramoğlu Yem, Erzurum Turkiye) for 16 weeks. Cafeteria Diet (CAF): fed with cafeteria diet for 16 weeks. Cafeteria Diet+7,8-DHF (7,8-DHF): fed cafeteria diet for 16 weeks. Last 28 days of feeding period 7,8-DHF was administered by i.p. injection 5 mg/kg/day. Sham: fed cafeteria diet for 16 weeks. Last 28 days of feeding period i.p. DMSO+PBS (solvent) was given by i.p. injection.

7,8-DHF (Cayman, USA) (5 mg/kg) was prepared by dissolving in PBS containing 17 % DMSO (dimethyl sulfoxide) [18] and administered to the 7,8-DHF and Sham group i.p. for 28 days.

The cafeteria diet used was prepared by modifying the diets in previous studies [19–21]. And a mixture of cafeteria diet and rodent diet (30 % rodent diet and 70 % CAF diet) was used (Table 1). Cafeteria diet containing less amounts of vitamins, minerals and trace elements. Hence, by adding normal rodent diet to cafeteria diet, the unwanted side effects related to above mentioned reason were avoided. Based on the energy values specified on the packaging of the foodstuffs used in the calculations. A diet adjustment was made ensuring that 40 % of energy intake was from fats, 55 % from carbohydrates and 5 % from protein.

During the 16-week diet program, the mice were weighed and recorded every second week. At the end of the diet protocol, the animals were sacrificed by decapitation. The trunk bloods were collected into a gel separation tube, serums were obtained and stored at −80 °C until the day of analysis. After the liver and pancreas tissues of the mice were removed, a piece was dissected and reserved for histopathological examinations. Rest of the collected tissues were placed in separate tubes for ELISA and qRT-PCR study and immediately frozen in liquid nitrogen. For expression studies, RNA was isolated on the same day from liver and pancreas tissues, cDNA was converted and stored at −80 °C. Epididymal adipose tissue (EAT) was removed and weighed. The % Adipocyte Index, which is a parameter of central obesity, was calculated ((EAT (g) / total body weight (g)) * 100) [22].

2.2. Measurement of serum biochemistry parameters

Glucose, triglyceride, cholesterol, alanine aminotransferase (ALT), and amylase levels in serum samples obtained from mice were measured

Table 1
Products used to obtain cafeteria diet and their energy contents (per 100 g).

	Energy (kcal)	Carbohydrate (g)	Fat (g)	Protein (g)
Hazelnut biscuit	470	64,2	19,5	7,8
Crackers	484	63	22	6,5
Fruit cake	378	56	14,9	4,2
Crisps	509,8	55,2	29,7	7,6
Chocolate wafer	517	63,1	26,9	5,8

in the Beckman Coulter Analyzer AU 5800 (California, USA) auto-analyzer available in the Medical Biochemistry Laboratory of Karadeniz Technical University Farabi Hospital.

2.3. Serum insulin and IL-1β levels

Insulin (Crystal Chem, USA) and IL-1β (Elabscience, USA) levels in serum were measured with commercial ELISA kits. Homeostatic Model Assessment of Insulin Resistance (HOMA-IR) value was calculated from insulin and glucose values by using the formula: (HOMA-IR = [insulin (μU/mL) × fasting glucose (mmol/L)] / 22.5) [23].

2.4. Oral Glucose Tolerance Test (OGTT)

At the end of the feeding period, OGTT was also performed on each mice to assess carbohydrate metabolism [24]. For the Oral Glucose Tolerance Test procedure, mice were fasted for 6 h (07.00–13.00 h) and fasting blood glucose (0 min) values were measured from tail vein blood with the help of a glucometer (Vital Plus G 400, Korea). Then, 2 g/kg glucose was given by gavage needle. Blood glucose values were measured with a glucometer at 30, 60, 90 and 120 min following glucose application.

2.5. CHOP and GRP78 levels in liver and pancreatic tissues

CHOP and GRP78 levels in liver and pancreas tissues were measured by ELISA method (Aviva, USA). Tissue homogenization and measurements were made in accordance with the manufacturer's recommendations. Results were expressed as ng/mg protein for CHOP and pg/mg protein for GRP78. Protein determination was performed using the BCA protein assay kit (Pierce^{Tm} Thermo Scientific, USA).

2.6. Liver triglyceride measurement

Triglyceride measurement in mouse liver tissue was performed by modifying the methods developed by Mopuri [25].and Choi [26]. Briefly, 25 mg of liver tissue was weighed and 500 μL of 1 M NaCl solution was added. It was then homogenized with a hand homogenizer (Omni Tissue Master 125, Kennesaw GA, USA). It was added 3 mL of chloroform/methanol (2,1) and incubated overnight in a shaker at room temperature. The homogenate was centrifuged at 3000 ×*g* for 10 min. The lower organic phase containing the lipid was transferred to a new tube. Excess liquid was evaporated in the oven at 500C. 200 μL of 1 M NaCl solution containing 2 % triton X-100 was added to dissolve the pellet. It was incubated for 15 min at room temperature. Then sonification was done 3 times for 5 s. The amount of triglycerides in the obtained solution was measured in an autoanalyzer (Beckman Coulter Analyzer AU 5800, California USA). Results are expressed per mg of protein. Protein determination was performed using the BCA protein assay kit (PierceTm Thermo Scientific, USA).

2.7. qRT-PCR

Total RNA isolation from liver and pancreas tissues was performed using TriPure Isolation reagent (Roche, Lot No. 11667157001, Switzerland) in accordance with the manufacturer's recommendations. Total RNAs obtained were translated into cDNA using the Transcriptor First Strand cDNA Synthesis kit (Roche, LotNo. 04896866001, Switzerland). CHOP (Ddit3) and GRP78 (Hspa5) gene expressions were performed on Light Cycler® 480 II system (Roche,Switzerland) device using LC FS DNA Master SYBR Green I kit (Roche, Switzerland). qRT-PCR reactions were run as a double reaction. Relative gene expressions were normalized to β-Actin and expression results were calculated using the method developed by Livak and Schmittgen [27]. The primer sequences of the target and reference genes are given in Table 2.

Table 2
Primer sequences used in RT-PCR.

Name of primer		Primer sequence
β-Aktin (Actb)	Forward primer	5′-CCG TAA AGA CCT CTA TGC CAA C-3′
	Reverse primer	5′-ACC GAT CCA CAC AGA GTA CTT G-3′
GRP78 (Hspa5)	Forward primer	5′-AGA GCC TTG TCT TCT CAG CAT C-3′
	Reverse primer	5′-CAA CAC TTT CTG GAC AGG CTT C-3′
CHOP (Ddit3)	Forward primer	5′-CAA GCA TGA ACA GTG GGC ATC-3′
	Reverse primer	5′-TGT ACC GTC TAT GTG CAA GCC-3′

2.8. Histological analysis

2.8.1. Histopathological evaluation of liver, pancreas and adipose tissues

At the end of the study, liver, pancreas and adipose tissue samples of the animals were fixed in 10 % formaldehyde solution for 48 h for light microscopic examination. Sections of 4–5 μm thickness from paraffin blocks were taken on slides for light microscopic methods with a fully automatic microtome (Leica RM 2255, Tokyo, Japan). Sections were stained with Hematoxylin-Eosin (H-E) staining method to observe the general histological structure. The obtained preparations were evaluated by an experienced histologist who was unaware of the study groups. Olympus BX51 (Olympus, Tokyo, Japan) microscope was used to evaluate the preparations. The findings were photographed with a light microscope-adapted camera attachment (Olympus DP71; Olympus, Tokyo, Japan). In the evaluation of the pancreas, the general histological structure and islet morphology of the pancreas were evaluated by Hematoxylin-Eosin staining. General pancreatic structure, vascular congestion, hemorrhage, inflammatory cell infiltration, edema and other degenerative changes were evaluated. The difference between the groups was investigated by taking the average of the analysis made on at least 10 images taken from different regions in each section under the light microscope [28]. In the histopathological evaluation of liver tissues; liver sections were evaluated semi-quantitatively in terms of hepatocyte degeneration, vascular congestion, sinusoidal dilatation, and congestion in enlarged sinusoids [29]. Semi-quantitative evaluation was performed as 0 = absent, 1 = mild, 2 = moderate, 3 = severe. In the evaluation of adipose tissues, the dimensions of fat cells and the tissue between fat cells were evaluated histopathologically. For adipose tissue, 10 images of each experimental group were photographed using a 10× objective [30].

2.8.2. Examination of TUNEL assay

In order to evaluate apoptosis in tissues, TUNEL (deoxynucleotidyl transferase (TdT) deoxyuridine triphospate nick end labeling assay) was used in accordance with the kit staining protocol. TUNEL (+) cells with homogeneously stained brown nuclei without areas of necrosis were defined as apoptotic cells. 3,3′-Diaminobenzidine (DAB) Enhanced Liquid Substrate System tetrahydrochloride was used to show apoptotic cells, and Mayer's hematoxylin was used for counterstaining. Apoptosis was evaluated in hepatocytes in the liver and Langerhans islet cells in the pancreas. In the evaluation, apoptotic and normal cells were recorded by counting 100 cells with Analysis 5 Research program (Olympus Soft Imaging Solutions, Münster, Germany) in 5 different areas at X400 magnification, and the percent apoptotic index (AI) was calculated (% AI = (TUNEL (+) cell number / total cell number) × 100) [31].

2.9. Statistical analysis

Weight, OGTT, q-RT-PCR and morphological change scores data were expressed as mean ± standard error (mean ± SE). Other data were given in [median (IQR)] quartiles of 25–75 %. The graphics were shaped as boxplot. Statistical difference between groups was determined by Kruskal Wallis analysis of variance. Pairwise comparisons between groups were made with the Mann–Whitney *U* test. $p < 0.05$ was considered statistically significant.

3. Results

3.1. Effect of 7,8-DHF on body weight, EAT and % Adipocyte Index

From the first four weeks of the experiment, the body weights of mice in CAF group significantly increased compared to the control group ($p < 0.01$) (Fig. 1). At the end of the experiment, the weights of the 7,8-DHF group decreased significantly compared to the CAF and Sham groups ($p < 0.05$) (Table 3). EAT and % Adipocyte Index values were significantly increased in the CAF group compared to the control group ($p < 0.01$). The EAT and % Adipocyte Index values of the 7,8-DHF group were significantly decreased compared to the CAF and Sham groups ($p < 0.05$) (Table 3). In EAT histopathological analysis, adipocytes in the CAF group were larger and rounder than the control group. Capillaries and vasocongestion were observed between adipocytes. In the 7,8-DHF group, the fat cells showed similar morphology to the control group, and capillaries showing occasional vasocongestion were observed between the fat cells (Fig. 2).

3.2. Effect of 7,8-DHF on serum biochemistry parameters and insulin and IL-1β levels

Serum triglyceride, cholesterol, amylase, ALT and glucose were analyzed to examine the general metabolic status (Table 4). Triglyceride, cholesterol, amylase, ALT and glucose levels were significantly higher in the CAF group compared to the control group ($p < 0.05$). Triglyceride, cholesterol, amylase, ALT and glucose values were significantly lower in the 7,8-DHF group compared to the CAF group ($p < 0.05$). Levels of insulin were examined to determine insulin resistance and IL-1β levels to assess inflammatory status. While HOMA-IR, IL-1β values were significantly higher in all groups compared to the control group ($p < 0.05$), HOMA-IR and IL-1β values were significantly lower in the 7,8-DHF group compared to the CAF group ($p < 0.05$).

3.3. Effect of 7,8-DHF on oral glucose tolerance

At the end of the diet protocol, OGTT procedure was applied to the animals. The changes in blood glucose were summarized in Fig. 3A and the areas under the curve (AUC) are given in Fig. 3B. Glucose values were found to be significantly higher in the CAF group compared to the control group in all measurements ($p < 0.01$). Glucose values were found to be significantly higher in the 7,8-DHF group compared to the control group in the initial and 30th minute measurements, while this difference disappeared at the 60th, 90th, and 120th minutes, and the mice showed normal glucose tolerance. In addition, it was found to be significantly lower in all measurements in the 7,8-DHF group than in the CAF group ($p < 0.05$). 7,8-DHF recued the impaired oral glucose tolerance.

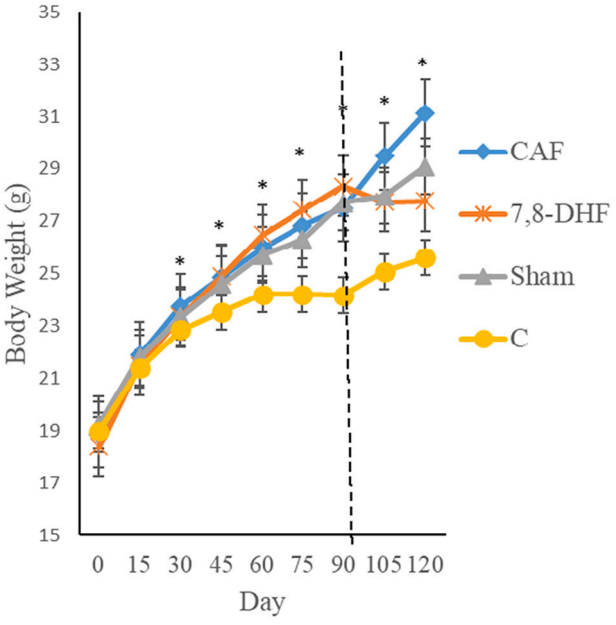


Fig. 1. Weight gains during 16 weeks diet protocols. *$p < 0.01$ compared with control group. *Dot line = Day for 7,8-DHF application.

Table 3
Body weights and EAT and % Adipocyte Index values of the groups.

	C	CAF	7,8-DHF	Sham
Initial body weight (g)	[18,90 (1,42)] 18,13–19,55	[18,70 (1,25)] 18,25–19,50	[18,30 (1,67)] 17,53–19,20	[19,75 (1,85)] 18,30–20,15
Final body weight (g)	[25,45 (2,67)] 24,75–27,42	[31,15 (2,83)][1] 29,80–32,63	[28,15 (1,95)][1,2] 26,83–28,78	[29,15 (1,15)][1,2,3] 28,63–29,78
Epididymal Fat Tissue weight (g)	[0,40 (0,13)] 0,30–0,42	[1,20 (0,47)][1] 1,05–1,52	[0,75 (0,23)][1,2] 0,67–0,90	[0,95 (0,33)][1,2,3] 0,77–1,12
% Adipocyte index	[1,51 (0,48)] 1,20–1,69	[3,76 (0,77)][1] 3,42–4,18	[2,62 (1,09)][1,2] 2,02–3,11	[3,29 (1,20)][1,3] 2,57–3,77

Values are given in [median (IQR)] quartiles of 25–75 %.
[1] $p < 0.05$ compare C group.
[2] $p < 0.05$ compare CAF group.
[3] $p < 0.05$ compare 7,8-DHF group.

3.4. Effect of 7,8-DHF on tissue GRP78 and CHOP protein levels

The GRP78 and CHOP concentrations of the groups are given in Fig. 4. In the liver tissue, GRP78 and CHOP protein levels, which are ERS biomarkers, were significantly increased in the CAF group compared to the control group ($p < 0.05$), while the increase in the pancreatic tissue was not statistically significant ($p > 0.05$). GRP78 and CHOP protein levels in liver tissue were significantly lower in the 7.8-DHF group compared to the CAF group ($p < 0.05$).

3.5. Findings related to expressions of genes measured in liver and pancreatic tissues

The plate was double-loaded for each gene from cDNAs obtained from liver and pancreas tissues of four groups. GRP78 (Hspa5) and CHOP (Ddit3) gene expressions were measured in these tissues by RT-PCR and crossing point (Cp, crossing point) values were obtained for each sample. Cp values obtained from the paired studies were averaged and fold changes were calculated for each group compared to the control group by using these Cp values. The results of GRP78 and CHOP gene expression are given in Fig. 5. GRP78 and CHOP gene expressions in liver tissue were found to be significantly higher in the CAF group compared to the control group, while only GRP78 levels were found to be significantly higher in pancreatic tissue ($p < 0.05$). In the 7,8-DHF group, GRP78 and CHOP levels were significantly reduced in liver tissue compared to the CAF group, and GRP78 levels in pancreatic tissue were significantly reduced ($p < 0.05$) (Fig. 5).

3.6. Effect of 7,8-DHF on liver triglyceride concentration

Liver triglyceride measurement was performed to show the lipid accumulation in the liver tissue. Results revealed that the lipid content was significantly increased in the CAF group compared to the control group ($p < 0.001$). On the other hand, 7,8-DHF significantly decreased liver lipid content compared to the CAF group ($p < 0.01$) (Table 4).

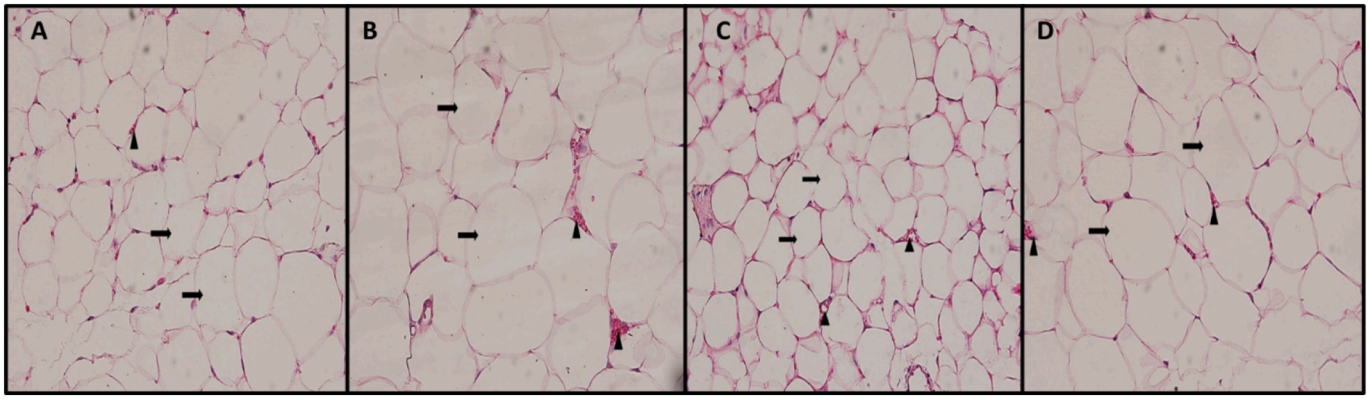


Fig. 2. A micrograph of lipid tissue. Arrow indicates a typical adipocyte. Triangel indicates vascular congestion (H&E X 200). A: C, B: CAF, C: 7,8-DHF, D: Sham.

Table 4
Serum biochemistry parameters, liver triglyceride insulin, HOMA-IR and IL-1β levels.

	C	CAF	7,8-DHF	Sham
Triglyceride (mg/dL)	[59,50 (14,50)] 50,50–65,00	[72,00 (9,00)][1] 69,50–78,50	[68,00 (16,00)][2] 55,50–71,50	[81 (24,00)][1,3] 69,50–93,50
Liver triglyceride (mg/mg protein)	[309,10 (105,3)] 240,85–346,15	[497,70 (116,5)][1] 425,75–542,52	[363,50 (99,5)][2] 308,90–408,40	[565,70 (134,95)][1,3] 511,15–646,10
Cholesterol (mg/dL)	[78,00 (9,50)] 69,50–79,00	[167,50 (17,50)][1] 159,00–176,50	[155,50 (18,50)][1,2] 149,50–168,00	[171,00 (28,50)][1,3] 163,50–192,00
Amylase (mg/dL)	[2021,00 (513)] 1650–2163	[2707 (69,00)]1 2657–2726	[2395 (206)][1,2] 2320–2527	[2720 (312)][1,3] 2600–2921
ALT (U/L)	[179,00 (31,50)] 157,00–188,50	[201,50 (76,5)][1] 184,00–260,50	[176,00 (14,25)][2] 169,25–183,50	[202,00 (18,25)][1,3] 190,00–208,25
Glucose (mg/dL)	[150,00 (29,50)] 144,50–175,00	[228,00 (15,00)][1] 216,00–231,00	[202,00 (27,00)][1,2] 192,00–219,00	[217,00 (9,50)][1,2] 210,50–220,00
Insulin (ng/mL)	[21,83 (8,97)] 16,80–25,77	[39,69 (23,94)][1] 26,23–50,17	[33,18 (13,13)][1] 22,99–36,12	[33,83 (15,67)][1] 31,81–47,48
HOMA-IR	[180,82 (81,02)] 142,23–223,25	[527,10 (315,8)][1] 322,53–638,32	[309,58 (204,96)][1,2] 242,70–447,66	[413,05 (441,42)][1] 372,01–813,43
IL-1β (pg/mL)	[638,01 (21,67)] 620,51–642,18	[971,31 (98,66)][1] 939,56–1038,22	[867,11 (82,15)][1,2] 831,60–913,75	[944,65 (236,83)][1] 806,57–1043,40

Data are given in [median (IQR)] quartiles of 25–75 %.
[1] $p < 0.05$ compare control group.
[2] $p < 0.05$ compare CAF group.
[3] $p < 0.05$ compare 7,8-DHF group.

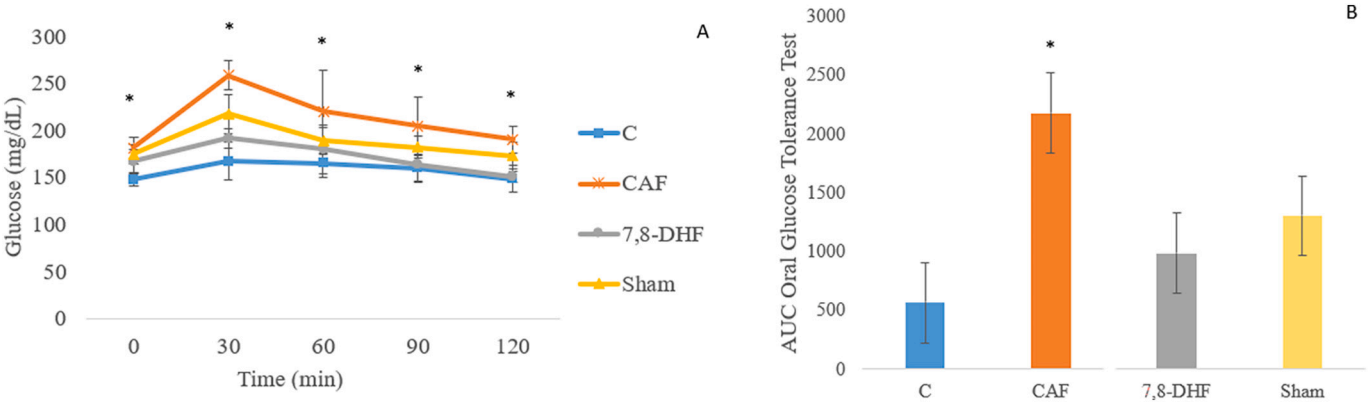


Fig. 3. A. OGTT *$p < 0.05$ compared with control group. B. Area Under Curve for OGTT.

3.7. *Effect of 7,8-DHF on histopathological parameters*

The data obtained from the light microscopy. Evaluation of the pancreatic tissues of the groups are given in Fig. 6 and the scorings are given in Table 5. Normal pancreatic serous acini and islet structure were observed in the control group (Fig. 6A). Pancreatic islet cells of Langerhans were observed in the normal structure in the CAF group. Widespread degeneration of pancreatic serous acini cells, inflammatory cell infiltration in the interlobular area, intraductal edema, and vascular congestion in intralobular vessels were observed (Fig. 6B). In the 7,8-DHF group, pancreatic islet cells of Langerhans and pancreatic serous acini cells were observed in normal structure. Mild intravascular

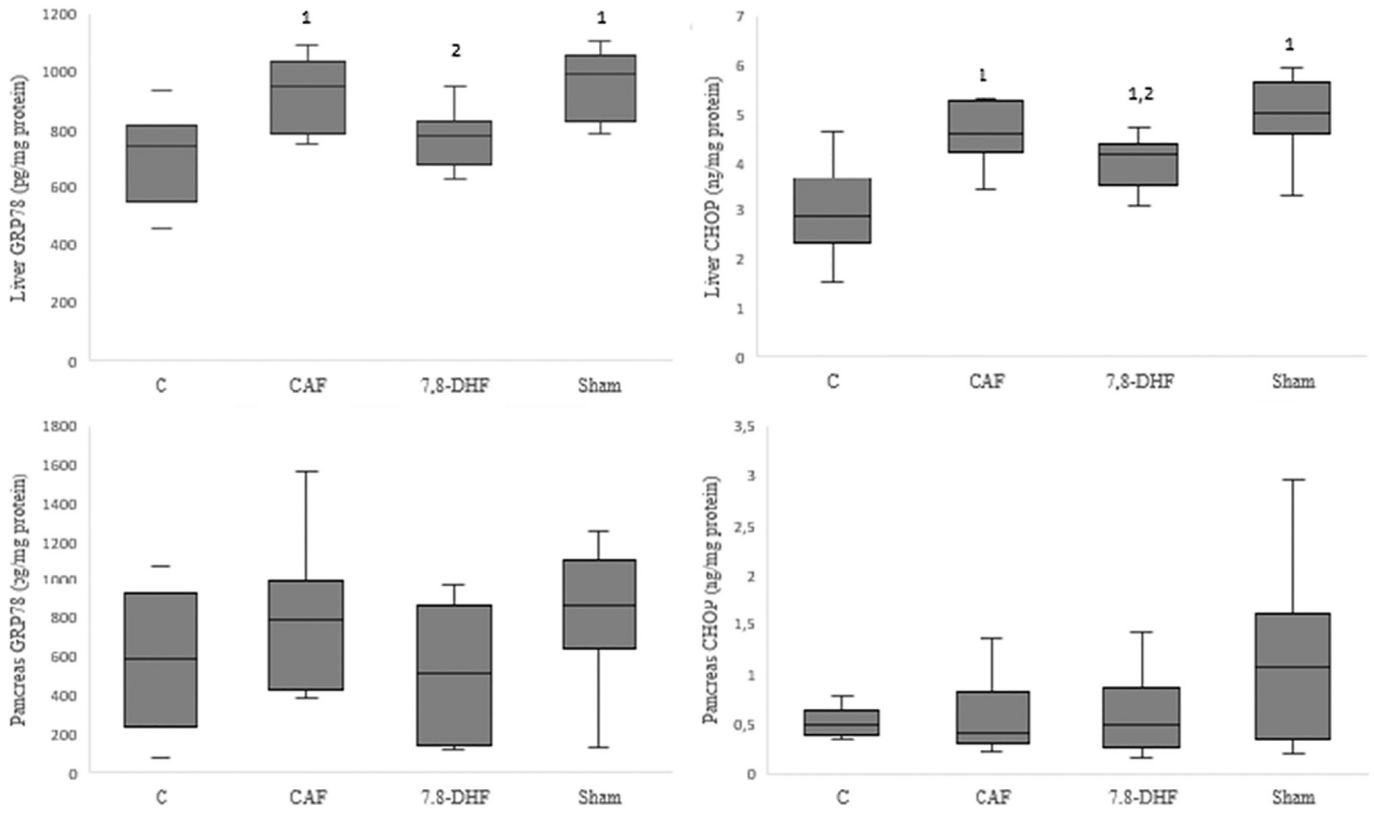


Fig. 4. GRP78 and CHOP levels of liver and pancreatic tissues.
[1]p < 0.05 compare control group.
[2]p < 0.05 compare CAF group.

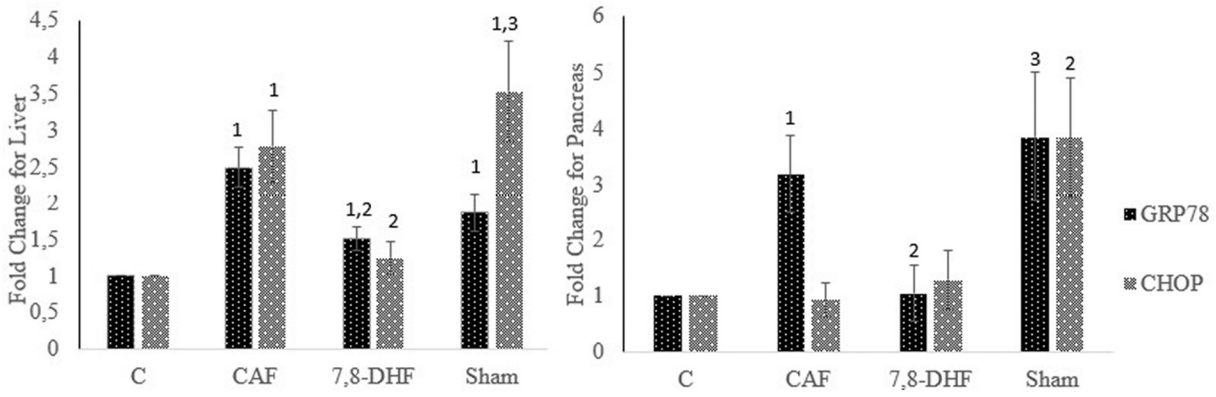


Fig. 5. Results of GRP78 and CHOP gene expression in liver and pancreas tissues.
[1]p < 0.05 compared to Control group.
[2]p < 0.05 compared to CAF group.
[3]p < 0.05 compared to 7,8-DHF group.

congestion and occasional mild intraductal edema were observed in the intralobular vessels (Fig. 6C). Pancreatic islet cells of Langerhans were observed in normal structure in the sham group. Moderate degeneration of pancreatic serous acini cells, intraductal edema and vascular congestion in intralobular vessels were observed (Fig. 6D).

Sample light microscopic photographs of liver are given in Fig. 7. The scorings of liver tissues are given in Table 6. Normal liver tissue morphology was observed in the control group. Hepatocytes and sinusoidal space were normal in appearance (Fig. 7A). Degeneration of hepatocytes and enlargement of the sinusoidal space were observed around the vena centralis in the CAF group (Fig. 7B). In the 7,8-DHF group, there are normal hepatocytes around the vena centralis. In areas far from the vena centralis, degeneration and sinusoidal spaces in hepatocytes were observed in normal morphology (Fig. 7C). In the sham group, degeneration of hepatocytes and enlargement of the sinusoidal space were observed around the vena centralis (Fig. 7D).

3.7.1. *Effect of 7,8-DHF on apoptosis*

Apoptosis evaluation of pancreatic islet cells of langerhans is given in Fig. 8 and Table 7, apoptosis evaluation of hepatocytes in liver is given in Fig. 9 and Table 7. given. A significant increase was found in all groups compared to the control group ($p < 0.001$). A significant

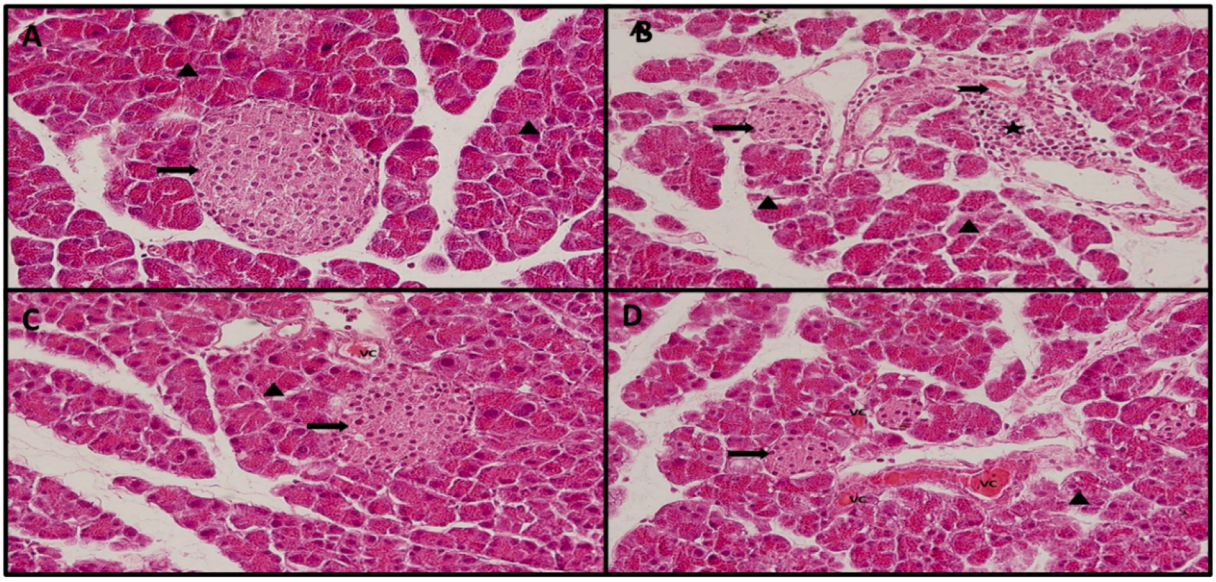


Fig. 6. Photomicrograph of the pancreas. Serous acini (Arrowhead), Langerhans islets (Arrow), inflammatory cell infiltration (star), intraductal edema (notched arrow), vascular congestion (VC) (H&E X 200). A: Control, B: CAF, C: 7,8-DHF, D: Sham.

Table 5
Morphological change scores of pancreatic tissue.

Pancreas	C	CAF	7,8-DHF	Sham
Vascular congestion	0,30 ± 0,15	1,90 ± 0,23[1]	1,20 ± 0,16[1,2]	1,50 ± 0,16[1]
Hemorrhage	0,10 ± 0,10	0,30 ± 0,15	0,30 ± 0,15	0,50 ± 0,16
Inflammatory cell infiltration	0,20 ± 0,13	2,00 ± 0,14[1]	0,60 ± 0,16[2]	1,00 ± 0,21[1,2]
Edema	0,10 ± 0,10	2,30 ± 0,15[1]	0,50 ± 0,16[2]	0,80 ± 0,13[1,2]

Data expressed as mean ± standard error (mean ± SE).
[1] $p < 0.05$ compared to Control group.
[2] $p < 0.05$ compared to CAF group.

decrease was found in the 7,8-DHF group compared to both CAF and Sham groups ($p < 0.01$). It can be suggested that 7,8-DHF significantly reduces the number of apoptotic cells.

4. Discussion

Current preclinical and clinical evidences confirm that prolonged ERS increases the risk of various metabolic disorders, including diabetes, obesity, and dyslipidemia [32]. Several naturally occurring and synthetic molecules have been identified for their efficacy in ameliorating ERS in both *in vitro* and *in vivo* models of metabolic disorders. Many compounds such as tauroursodeoxycholate, quercetin, elatoside, sulforaphane, and berberine have shown to reduce ERS in various ways [33–37]. In this study, we demonstrated that 7,8-DHF, which has various biological properties such as antioxidant and anti-apoptotic effects as well as acts as BDNF mimetic, suppresses ERS in liver and pancreatic tissues and rescues metabolic changes caused by ERS in a

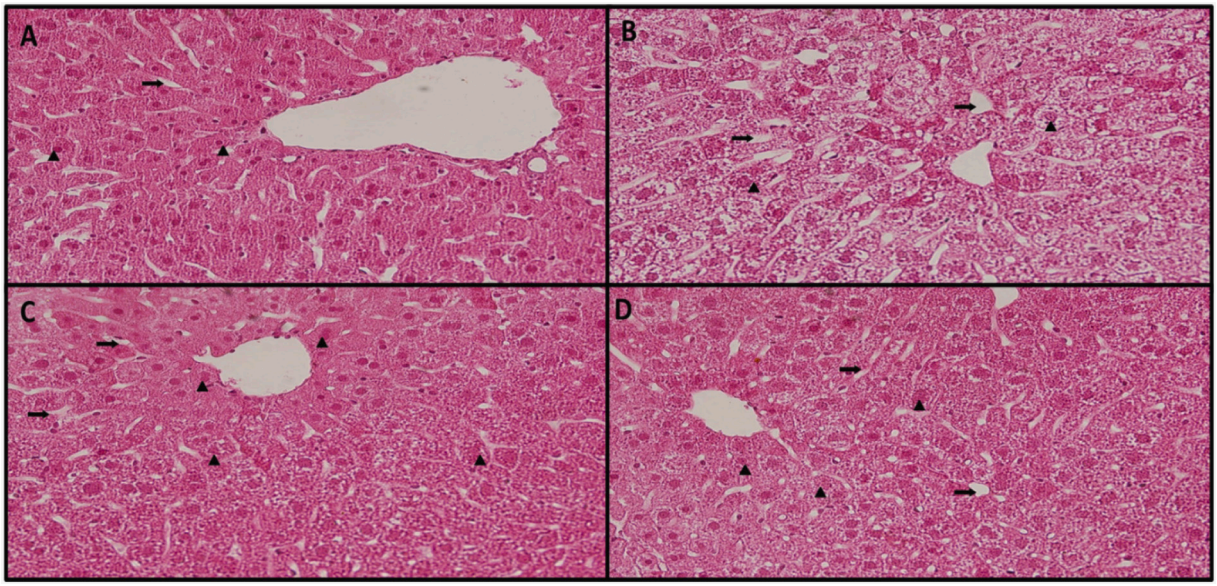


Fig. 7. Photomicrograph of the liver tissues. Hepatocyte (arrow head), Sinusoidal dilatation (arrow) (H&E X 200). A: Control, B: CAF, C: 7,8-DHF, D: Sham.

Table 6
Morphological change scores of liver tissue.

Liver	C	CAF	7,8-DHF	Sham
Vascular congestion	0,30 ± 0,15	2,60 ± 0,16[1]	1,40 ± 0,16[1,2]	2,30 ± 0,21[1,3]
Hemorrhage	1,00 ± 0,14	1,30 ± 0,15	1,50 ± 0,16	1,50 ± 0,16[1]
Inflammatory cell infiltration	1,50 ± 0,22	2,10 ± 0,17[1]	1,60 ± 0,16	1,80 ± 0,13
Edema	0,80 ± 0,13	1,40 ± 0,16[1]	1,10 ± 0,10	1,20 ± 0,13

Data expressed as mean ± standard error (mean ± SE).
[1] $p < 0.05$ compared to Control group.
[2] $p < 0.05$ compared to CAF group.
[3] $p < 0.05$ compared to 7,8-DHF group.

mouse metabolic syndrome model induced by CAF diet. We showed that the CAF diet we used in our study significantly increased the total body weight, epididymal adipose tissue amount, % adipocyte index, serum triglyceride, cholesterol and glucose values of the mice ($p < 0.05$). The development of metabolic syndrome in C57BL6/J mice is evaluated by the obesity, hyperglycemia and dyslipidemia observed in mice [38,39]. Our data verified that the CAF diet successfully induced metabolic syndrome in our experimental groups. In contrast, there was a significant decrease in the above-mentioned parameters in the group treated with 7,8-DHF ($p < 0.05$) (Table 3). Adipose tissue histological analysis revealed that mice in the CAF group, the epididymal fat accumulation had increased in parallel with the increased weight, resulting in adipocyte hypertrophy. However, there was no significant change in adipocyte structure in the 7,8-DHF group (Fig. 2). Wood et al. [40] showed that 7,8-DHF administration alleviated body weight gain by increasing muscle mitochondrial respiration and systemic energy expenditure, and partially reversed metabolic abnormalities caused by obesity. Our results also support this report, showing that 7,8-DHF reversed the metabolic changes induced by the CAF diet. ER stress and obesity create a vicious cycle. ER stress contributes to obesity, while obesity exacerbates ER stress. Although initially the UPR is an adaptive response to ER stress, hyperactivation of the UPR can become a maladaptive process in obesity. Therefore, new therapeutics that reduce ER stress and changes in eating and drinking habits may be effective in combating both ER stress and obesity. In this context, 7,8-DHF may be effective in breaking the vicious circle between ER stress and obesity by reducing adiposity [41].

Insulin is synthesized as proinsulin in the ER of β-cells, than converted to its active form and stored in granules in the cell cytosol. Causes such as increased proinsulin synthesis and/or deterioration of Ca^{2+} homeostasis in the ER due to reasons such as chronic hyperglycemia and peripheral insulin resistance leads to the accumulation of unfolded and/or misfolded insulin in the ER lumen. This activates the UPR, which is an intracellular signaling pathway in β-cells, in order to restore the intracellular homeostasis. However, if the UPR is insufficient, ERS prolongs and eventually apoptotic cell death occurs. As a result, β-cells are lost [42]. Oxidative stress, ERS, and secretion of inflammatory cytokines play an important role in the pathogenesis of diabetes mellitus. It has been shown that ERS alone can initiate or exacerbate β-cell dysfunction and even initiate cell death [43]. To examine ER stress in pancreatic tissue, we investigated GRP78, a sensor of ER stress, and CHOP, a marker of apoptosis, mRNA expression and protein levels. The fact that the GRP78 mRNA expression results were significantly higher in the CAF group compared to the control group, while 7,8-DHF decreased this value compered to CAF group ($p < 0.05$) (Fig. 5). Again, histopathological analyzes support that 7,8-DHF ameliorates the damage caused by the CAF diet (Figs. 6, 8 and Table 7). Although we could not find a significant change in CHOP gene and protein levels, the high apoptotic index values we obtained in the CAF group compared to the control group ($p < 0.05$) (Table 7) as a result of TUNEL kit staining show that apoptosis occurs in this tissue. 7,8-DHF significantly reduced this value compered to CAF group ($p < 0.05$). There are alternative routes available [5] which may explain why we could not observe a difference

Table 7
Pancreas and liver apoptotic indexes.

%AI	C	CAF	7,8-DHF	Sham
Pancreas	[9,00 (3,50)] 7,75–11,25	[37,00 (9,00)][1] 31,25–40,25	[17,00 (5,75)][1,2] 12,5–18,25	[29,00 (6,00)][1,2,3] 25,25–31,25
Liver	[9,00 (2,50)] 8,75–11,25	[81,00 (10,00)][1] 73,50–83,50	[51,50 (8,50)][1,2] 49–57,50	[64,50 (8,50)][1,2,3] 60,50–69,00

Values are given in [median (IQR)] quartiles of 25–75 %.
[1] $p < 0.05$ compare control group.
[2] $p < 0.05$ compare CAF group.
[3] $p < 0.05$ compare 7,8-DHF group.

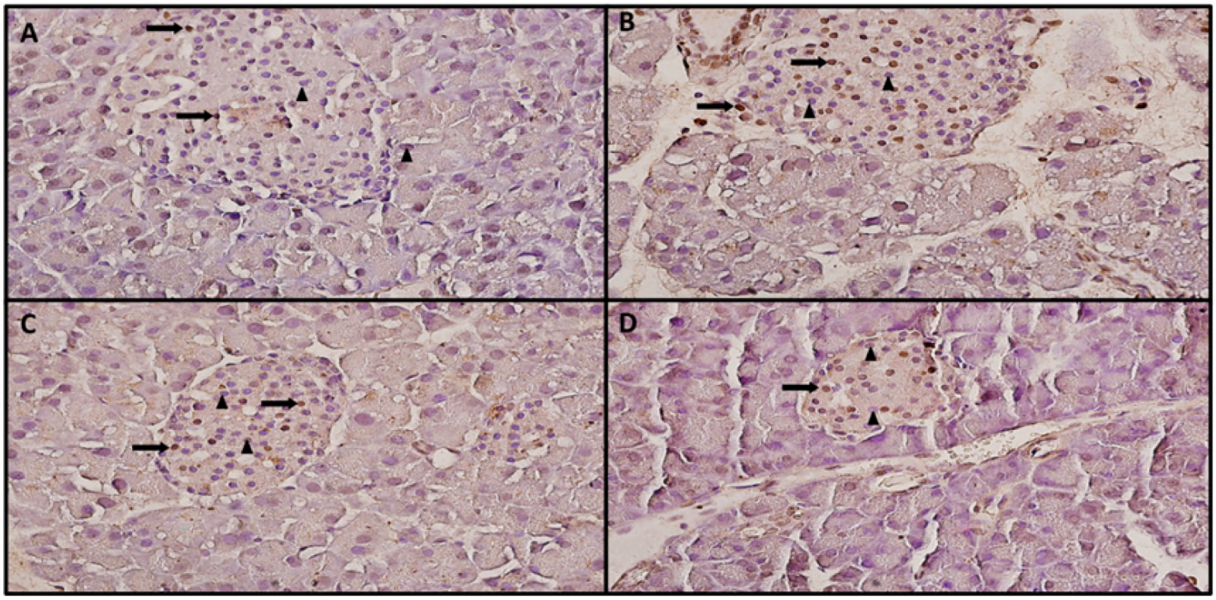


Fig. 8. Photomicrograph of the pancreas. TUNEL (−) cell (arrow head), TUNEL (+) cell (arrow) (TUNEL X 400) A: Control, B: CAF, C: 7,8-DHF, D: Sham.

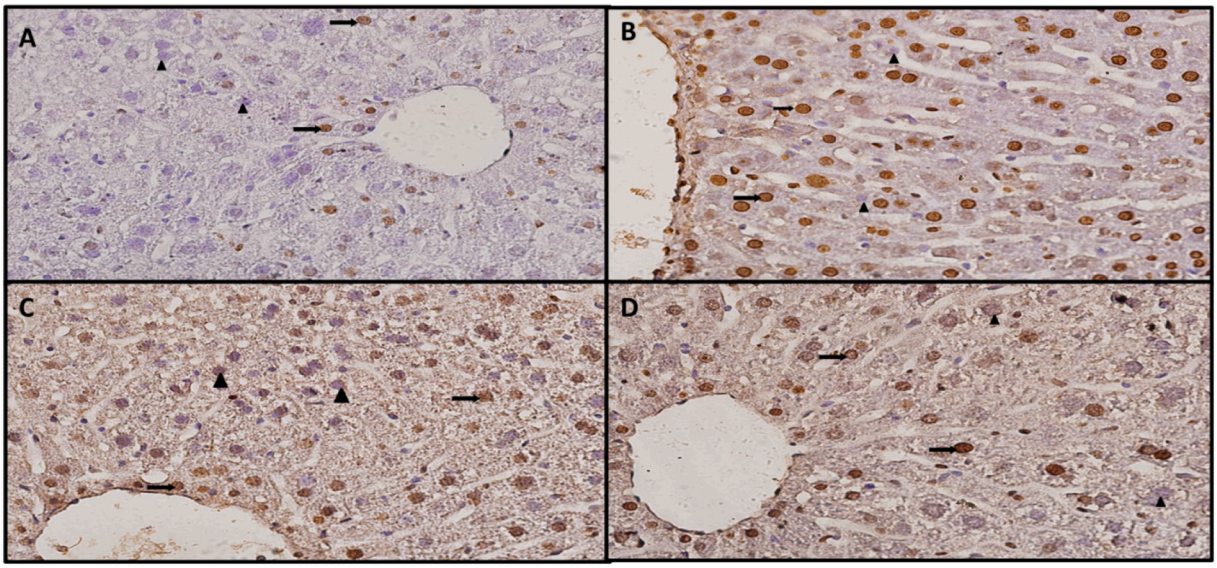


Fig. 9. Photomicrograph of the liver tissues. TUNEL (−) cell (arrow head), TUNEL (+) cell (arrow) (TUNEL X 400) A: Control, B: CAF, C: 7,8-DHF, D: Sham.

between CHOP levels inspite of elevated GRP78 and apoptosis. Also, depending on the long (16 weeks) feeding period, the CHOP levels may have increased and decreased to normal concentrations. In a recent study Yong et al. [44], showed that deletion of Chop/Ddit3, a marker of apoptosis, in pancreatic β cells alleviated ERS and reduced hepatic steatosis. In another study, Chop deletion was shown to reduce oxidative stress, improve β-cell function, and promote cell survival in a diabetic mouse model [45]. Adult human pancreatic islets exhibit little or no β-cell turnover. Therefore, interventions aimed at reducing ERS associated with proinsulin synthesis to preserve β-cell mass and insulin secretion function (*i.e.* 'functional β-cell mass') could be used to provide a novel T2DM therapy [46]. 7,8-DHF prevents β damage by reducing ERS and protecting cells from apoptosis. 7,8-DHF may have exerted this protective effect through mechanisms other than TrkB activation. Various studies have shown that 7,8-DHF may exert a potent antioxidant effect and protect different cells (retinal ganglion and RGC-5 cells, hippocampal HT-22 cells or Chinese hamster lung fibroblast cells) against oxidative damage caused by glutamate or H_2O_2 [14,47,48]. In a study, it was concluded that inhibition of the vascular endothelial growth factor receptor (VEGFR2), which is involved in many events in immunity, vascularization and cell migration, may be beneficial in T1DM by reducing insulitis and repairing islet function in NOD mice [49]. In another study, it was reported that 7,8-DHF binds to VEGFR2 and exerts an antagonistic effect [50]. The protective effects of 7,8-DHF in suppressing ERS and apoptosis in pancreatic tissue may at least partially attributed to VEGFR2 inhibition by 7,8-DHF.

One of the underlying mechanisms of obesity-associated insulin resistance and diabetes is the development of chronic low-grade inflammation. During ERS, the IRE1-XBP pathway activates TNF-α expression. At the same time, the PERK arm of ERS initiates the cellular inflammatory cascade through activation of the JNK pathway [51]. Finally, activated ATF6 activates IL6, TNF-α and NF-KB expression. It eventually inhibits the anti-inflammatory protein kinase B pathway [52]. Meanwhile, increased JNK also activates proinflammatory cytokines (IL6) and several chemokines, which are the main activators of macrophages in the circulation as well as in the vicinity of inflammation [53]. Macrophages then engulf the adipocytes, resulting in the formation of crown-like structures that are the hallmark of obesity. These structures activate lipolysis in adipocytes. As a result, free fatty acid levels increase and free fatty acids accumulating in the liver as well as in the muscles induce cellular dysfunction [54]. This is one of the main causes of fatty liver and cardiovascular diseases. This lipotoxicity damages the pancreas as well [55]. In our study, IL-1β level, which we found significantly higher in the CAF group (Table 4), is a separate indicator of ERS and the development of an inflammatory environment. 7,8-DHF also significantly reduced inflammation by suppressing ERS ($p < 0.05$). One of the hallmarks of metabolically unhealthy obese and/or individuals with prediabetes or early stage T2DM is chronic fasting hyperinsulinemia. Hyperinsulinemia and hyperinsulinemia induced ERS may contribute directly to the development of non-alcoholic fatty liver disease (NAFLD) through effects on hepatocyte lipid homeostasis and indirectly *via* adipocyte enlargement. The causal role of hyperinsulinemia in hepatic steatosis and subsequent T2DM is increasingly recognized [56]. We also observed hyperinsulinemia in the CAF group in our study. Accordingly, we found increased lipid accumulation and serum triglyceride and cholesterol levels in the liver tissue (Table 4). We also showed that GRP78 was significantly higher at both protein and gene levels in the liver CAF group ($P < 0.05$). Stress development in the ER, which is an important organelle for lipid synthesis, causes disruption of lipid homeostasis. As a result, IR develops in the liver [57]. IR initially mediates hyperglycemia during type 2 diabetes mellitus, but later insulin deficiency due to beta cell loss contributes to the development of the disease. In the liver, ERS causes IRE1-mediated JNK activation [58]. Activated JNK impairs insulin action by phosphorylating serine residues of insulin receptor substrates 1 and 2 [59]. Our HOMA-IR results show that 7,8-DHF reduces IR resistance and, accordingly, suppresses ERS in the liver (Table 4). In line with this finding, GRP78 levels are also low in this group (Figs. 4, 5). Similar efficacy of 7,8-DHF is observed in histological evaluation (Fig. 7, Table 6). The UPR pathway is a critical factor for initiation of hepatocyte death and a potential promoter of inflammation [60]. The significantly higher liver CHOP protein and gene expression in the CAF group are indications that the cell is directed to apoptosis after activated ERS (Figs. 4 and 5). This Notion is also supported by the high %AI values in histological analyzes (Table 7). In fatty liver, reactive oxygen species is mainly produced by CHOP protein [44]. 7,8-DHF may have protected cells from apoptosis by suppressing CHOP expression and protein levels, and by scavenging reactive oxygen species produced by CHOP with its antioxidant properties. Although the BDNF/TrkB pathway in the brain and its relationship with ER stress are known in more detail [61,62], the pathway in peripheral organs such as the pancreas and liver and its effects on ER stress have not been fully elucidated. In general, binding of BDNF to its specific receptor, TrkB, causes receptor dimerization and activation of adapter proteins. Adaptor proteins are involved in the activation of phosphoinositide 3-kinase

(PI3K)-AKT (PI3K-AKT), Ras-mitogen-activated protein kinase (Ras-MAPK), and phospholipase C1 (PLC-1)-protein kinase C (PKC) signaling pathways, respectively. Studies have shown that endogenous BDNF may play a protective role in the kidneys against apoptosis induced by ERS through the suppression of CHOP [63].Yet another study revealed that endogenous BDNF exerts protective effects against apoptosis through CHOP suppression and steatosis through SREBP-1c suppression during ER stress in liver tissue [64]. So, 7,8-DHF, a good BDNF mimetic and high-affinity TrkB agonist, may have reduced ER stress in CAF-diet-induced metabolic syndrome in pancreas and liver tissues through activation of the BDNF/TrkB pathway.

In this study, we observed changes in some parameters such as glucose and body weight that is associated with DMSO, which is used as the solvent 7,8-DHF (Figs. 2, 3 and Table 3). In a study, it was stated that DMSO increased the translocation of GLUT4, which is the glucose transporter responsible for glucose entry into tissues such as muscle and fat, to the membrane [65]. This may be the reason for the decrease in serum glucose values in the DMSO group. In addition, another study showed that DMSO inhibited the differentiation of 3T3L1 preadipocytes into adipocytes [66]. Although DMSO has a reduced these parameters, the curative effect of 7,8-DHF seems to be greater than DMSO is greater in all parameters. However, further studies are needed to fully understand the effects of DMSO, especially on carbohydrate metabolism.

5. Conclusion

It is now well known that chronic ERS is involved in the pathogenesis of many metabolic diseases such as diabetes, obesity, cardiovascular diseases, non-alcoholic fatty liver disease. Recent findings suggest that pharmacological inhibition of ERS may be beneficial for the treatment of various metabolic disorders. In the cafeteria diet-induced mouse metabolic syndrome model, 7,8-DHF suppressed ERS and ERS-induced metabolic disorders in both liver and pancreas through activation of the BDNF/TrkB pathway. Therefore, 7,8-DHF and its biochemical pathways carry a potential to develop novel therapeutic strategies for treatment of ERS and metabolic diseases caused by ERS.

Funding sources

This study was supported by the Scientific Research Projects Coordination Unit at the Karadeniz Technical University (Project Numbers: TDK-2020-8738 and THD-2021-9366).

CRediT authorship contribution statement

Elif Sahin: Investigation, Formal analysis, Methodology. **Neslihan Saglam:** Formal analysis. **Seniz Erdem:** Formal analysis. **Elif Alvuroglu:** Formal analysis. **Ismail Abidin:** Writing – original draft. **Esin Yulug:** Methodology, Formal analysis. **Ahmet Alver:** Supervision, Writing – original draft.

Declaration of competing interest

The authors report no conflicts of interest.

References

[1] M.G. Saklayen, The global epidemic of the metabolic syndrome, Curr. Hypertens. Rep. 20 (2) (2018) 12, https://doi.org/10.1007/s11906-018-0812-z.
[2] E. McCracken, M. Monaghan, S. Sreenivasan, Pathophysiology of the metabolic syndrome, Clin. Dermatol. 36 (1) (2018) 14–20, https://doi.org/10.1016/j.clindermatol.2017.09.004.
[3] R. Bravo, V. Parra, D. Gatica, A.E. Rodriguez, N. Torrealba, F. Paredes, Z.V. Wang, A. Zorzano, J.A. Hill, E. Jaimovich, A.F. Quest, S. Lavandero, Endoplasmic reticulum and the unfolded protein response: dynamics and metabolic integration, Int. Rev. Cell Mol. Biol. 301 (2013) 215–290, https://doi.org/10.1016/B978-0-12-407704-1.00005-1.
[4] D.S. Schwarz, M.D. Blower, The endoplasmic reticulum: structure, function and response to cellular signaling, Cell. Mol. Life Sci. 73 (1) (2016) 79–94, https://doi.org/10.1007/s00018-015-2052-6.
[5] R. Ghemrawi, S.F. Battaglia-Hsu, C. Arnold, Endoplasmic reticulum stress in metabolic disorders, Cells 7 (6) (2018) 63, https://doi.org/10.3390/cells7060063.
[6] S.W. Jang, X. Liu, M. Yepes, K.R. Shepherd, G.W. Miller, Y. Liu, W.D. Wilson, G. Xiao, B. Blanchi, Y.E. Sun, K. Ye, A selective TrkB agonist with potent neurotrophic activities by 7,8-dihydroxyflavone, Proc. Natl. Acad. Sci. U. S. A. 107 (6) (2010) 2687–2692, https://doi.org/10.1073/pnas.0913572107.
[7] H. Rosas-Vargas, J.D. Martínez-Ezquerro, T. Bienvenu, Brain-derived neurotrophic factor, food intake regulation, and obesity, Arch. Med. Res. 42 (6) (2011) 482–494, https://doi.org/10.1016/j.arcmed.2011.09.005.
[8] A. Tsuchida, T. Nonomura, T. Nakagawa, Y. Itakura, M. Ono-Kishino, M. Yamanaka, E. Sugaru, M. Taiji, H. Noguchi, Brain-derived neurotrophic factor ameliorates lipid metabolism in diabetic mice, Diabetes Obes. Metab. 4 (4) (2002) 262–269, https://doi.org/10.1046/j.1463-1326.2002.00206.x.
[9] C. Chen, Z. Wang, Z. Zhang, X. Liu, S.S. Kang, Y. Zhang, K. Ye, The prodrug of 7,8-dihydroxyflavone development and therapeutic efficacy for treating Alzheimer's disease, Proc. Natl. Acad. Sci. U. S. A. 115 (3) (2018) 578–583, https://doi.org/10.1073/pnas.1718683115.
[10] M. Wurzelmann, J. Romeika, D. Sun, Therapeutic potential of brain-derived neurotrophic factor (BDNF) and a small molecular mimics of BDNF for traumatic brain injury, Neural Regen. Res. 12 (1) (2017) 7–12, https://doi.org/10.4103/1673-5374.198964.
[11] J.W. Choi, C.W. Lee, J. Lee, D.J. Choi, J.K. Sohng, Y.I. Park, 7,8-Dihydroxyflavone inhibits adipocyte differentiation via antioxidant activity and induces apoptosis in 3T3-L1 preadipocyte cells, Life Sci. 144 (2016) 103–112, https://doi.org/10.1016/j.lfs.2015.11.028.
[12] C.B. Chan, M.C. Tse, X. Liu, S. Zhang, R. Schmidt, R. Otten, L. Liu, K. Ye, Activation of muscular TrkB by its small molecular agonist 7,8-dihydroxyflavone sex-dependently regulates energy metabolism in diet-induced obese mice, Chem. Biol. 22 (3) (2015) 355–368, https://doi.org/10.1016/j.chembiol.2015.02.003.
[13] J. Wood, M. Tse, X. Yang, D. Brobst, Z. Liu, B. Pang, W.S. Chan, A.M. Zaw, B. Chow, K. Ye, C.W. Lee, C.B. Chan, BDNF mimetic alleviates body weight gain in obese mice by enhancing mitochondrial biogenesis in skeletal muscle, Metab. Clin. Exp. 87 (2018) 113–122, https://doi.org/10.1016/j.metabol.2018.06.007.
[14] V.K. Gupta, Y. You, J.C. Li, A. Klistorner, S.L. Graham, Protective effects of 7,8-dihydroxyflavone on retinal ganglion and RGC-5 cells against excitotoxic and oxidative stress, J. Mol. Neurosci. 49 (1) (2013) 96–104, https://doi.org/10.1007/s12031-012-9899-x.
[15] J.S. Kang, I.W. Choi, M.H. Han, G.Y. Kim, S.H. Hong, C. Park, H.J. Hwang, C. M. Kim, B.W. Kim, Y.H. Choi, The cytoprotective effects of 7,8-dihydroxyflavone against oxidative stress are mediated by the upregulation of Nrf2-dependent HO-1 expression through the activation of the PI3K/Akt and ERK pathways in C2C12 myoblasts, Int. J. Mol. Med. 36 (2) (2015) 501–510, https://doi.org/10.3892/ijmm.2015.2256.
[16] B. Wang, Q. Zhang, R. Yao, X. Liu, Z. Qu, 7, 8-Dihydroxyflavone protects an endothelial cell line from H_2O_2 damage, PLoS One 10 (8) (2015), e0135345, https://doi.org/10.1371/journal.pone.0135345.
[17] R. Ma, J. Zhang, X. Liu, S. Yue, Q. Zhao, Y. Xu, 7,8-DHF treatment induces Cyr61 expression to suppress hypoxia induced ER stress in HK-2 cells, Biomed. Res. Int. 2016 (2016) 5029797, https://doi.org/10.1155/2016/5029797.
[18] Y. Zeng, F. Lv, L. Li, H. Yu, M. Dong, Q. Fu, 7,8-Dihydroxyflavone rescues spatial memory and synaptic plasticity in cognitively impaired aged rats, J. Neurochem. 122 (4) (2012) 800–811, https://doi.org/10.1111/j.1471-4159.2012.07830.x.
[19] K. Holemans, S. Caluwaerts, L. Poston, F.A. Van Assche, Diet-induced obesity in the rat: a model for gestational diabetes mellitus, Am. J. Obstet. Gynecol. 190 (3) (2004) 858–865, https://doi.org/10.1016/j.ajog.2003.09.025.
[20] B.P. Sampey, A.M. Vanhoose, H.M. Winfield, A.J. Freemerman, M.J. Muehlbauer, P.T. Fueger, C.B. Newgard, L. Makowski, Cafeteria diet is a robust model of human metabolic syndrome with liver and adipose inflammation: comparison to high-fat diet, Obesity (Silver Spring, Md.) 19 (6) (2011) 1109–1117, https://doi.org/10.1038/oby.2011.18.
[21] Y. Buyukdere, A. Gulec, A. Akyol, Cafeteria diet increased adiposity in comparison to high fat diet in young male rats, PeerJ 7 (2019), e6656, https://doi.org/10.7717/peerj.6656.
[22] M.C. Della Vedova, M.D. Muñoz, L.D. Santillan, M.G. Plateo-Pignatari, M. J. Germanó, M.E. Rinaldi Tosi, S. Garcia, N.N. Gomez, M.W. Fornes, S.E. Gomez Mejiba, D.C. Ramirez, A mouse model of diet-induced obesity resembling most features of human metabolic syndrome, Nutr. Metab. Insights 9 (2016) 93–102, https://doi.org/10.4137/NMI.S32907.
[23] M.K. Garg, M.K. Dutta, N. Mahalle, Study of beta-cell function (by HOMA model) in metabolic syndrome, Indian J. Endocrinol. Metab. 15 (Suppl. 1) (2011) S44–S49, https://doi.org/10.4103/2230-8210.83059.
[24] R. Faulhaber-Walter, W. Jou, D. Mizel, L. Li, J. Zhang, S.M. Kim, Y. Huang, M. Chen, J.P. Briggs, O. Gavrilova, J.B. Schnermann, Impaired glucose tolerance in the absence of adenosine A1 receptor signaling, Diabetes 60 (10) (2011) 2578–2587, https://doi.org/10.2337/db11-0058.
[25] R. Mopuri, M. Kalyesubula, A. Rosov, N. Edery, U. Moallem, H. Dvir, Improved Folch method for liver-fat quantification, Front. Vet. Sci. 7 (2021) 594853, https://doi.org/10.3389/fvets.2020.594853.
[26] K.M. Choi, Y.S. Lee, D.M. Shin, S. Lee, K.S. Yoo, M.K. Lee, J.H. Lee, S.Y. Kim, Y. M. Lee, J.T. Hong, Y.P. Yun, H.S. Yoo, Green tomato extract attenuates high-fat-diet-induced obesity through activation of the AMPK pathway in C57BL/6 mice, J. Nutr. Biochem. 24 (1) (2013) 335–342, https://doi.org/10.1016/j.jnutbio.2012.06.018.

[27] K.J. Livak, T.D. Schmittgen, Analysis of relative gene expression data using real-time quantitative PCR and the 2(-Delta Delta C(T)) Method, Methods (San Diego, Calif.) 25 (4) (2001) 402–408, https://doi.org/10.1006/meth.2001.1262.
[28] S. Sag, M. Imamoglu, H. Sarihan, E. Yulug, A. Alver, S. Geze Saatci, A. Cay, Effects of carbon dioxide pneumoperitoneum on exocrine and endocrine functions, and oxidative state of rat pancreas, Biotech. Histochem. 96 (4) (2021) 257–262, https://doi.org/10.1080/10520295.2020.1789224.
[29] Ö. Saral, O. Yildiz, R. Aliyazicioğlu, E. Yuluğ, S. Canpolat, F. Öztürk, S. Kolayli, Apitherapy products enhance the recovery of CCL4-induced hepatic damages in rats, Turk. J. Med. Sci. 46 (1) (2016) 194–202, https://doi.org/10.3906/sag-1411-35.
[30] A. De Faveri, R. De Faveri, M.F. Broering, I.T. Bousfield, M.J. Goss, S.P. Muller, R. O. Pereira, E. de Oliveira, A.M. Silva, I.D. Machado, N. Quintão, J.R. Santin, Effects of passion fruit peel flour (Passiflora edulis f. flavicarpa O. Deg.) in cafeteria diet-induced metabolic disorders, J. Ethnopharmacol. 250 (2020), 112482, https://doi.org/10.1016/j.jep.2019.112482.
[31] O. Yıldız, Z. Can, O. Saral, E. Yuluğ, F. Oztürk, R. Aliyazıcıoğlu, S. Canpolat, S. Kolaylı, Hepatoprotective potential of chestnut bee pollen on carbon tetrachloride-induced hepatic damages in rats, Evid. Based Complement. Alternat. Med. 2013 (2013) 461478, https://doi.org/10.1155/2013/461478.
[32] R. Ghemrawi, S.F. Battaglia-Hsu, C. Arnold, Endoplasmic reticulum stress in metabolic disorders, Cells 7 (6) (2018) 63, https://doi.org/10.3390/cells7060063.
[33] M. Kars, L. Yang, M.F. Gregor, B.S. Mohammed, T.A. Pietka, B.N. Finck, B. W. Patterson, J.D. Horton, B. Mittendorfer, G.S. Hotamisligil, S. Klein, Tauroursodeoxycholic acid may improve liver and muscle but not adipose tissue insulin sensitivity in obese men and women, Diabetes 59 (8) (2010) 1899–1905, https://doi.org/10.2337/db10-0308.
[34] N. Suganya, E. Bhakkiyalakshmi, S. Suriyanarayanan, R. Paulmurugan, K. M. Ramkumar, Quercetin ameliorates tunicamycin-induced endoplasmic reticulum stress in endothelial cells, Cell Prolif. 47 (3) (2014) 231–240, https://doi.org/10.1111/cpr.12102.
[35] M. Wang, X.B. Meng, Y.L. Yu, G.B. Sun, X.D. Xu, X.P. Zhang, X. Dong, J.X. Ye, H. B. Xu, Y.F. Sun, X.B. Sun, Elatoside C protects against hypoxia/reoxygenation-induced apoptosis in H9c2 cardiomyocytes through the reduction of endoplasmic reticulum stress partially depending on STAT3 activation, Apoptosis 19 (12) (2014) 1727–1735, https://doi.org/10.1007/s10495-014-1039-3.
[36] C.A. Danilov, K. Chandrasekaran, J. Racz, L. Soane, C. Zielke, G. Fiskum, Sulforaphane protects astrocytes against oxidative stress and delayed death caused by oxygen and glucose deprivation, Glia 57 (6) (2009) 645–656, https://doi.org/10.1002/glia.20793.
[37] G.L. Zhao, L.M. Yu, W.L. Gao, W.X. Duan, B. Jiang, X.D. Liu, B. Zhang, Z.H. Liu, M. E. Zhai, Z.X. Jin, S.Q. Yu, Y. Wang, Berberine protects rat heart from ischemia/reperfusion injury via activating JAK2/STAT3 signaling and attenuating endoplasmic reticulum stress, Acta Pharmacol. Sin. 37 (3) (2016) 354–367, https://doi.org/10.1038/aps.2015.136.
[38] S.K. Wong, K.Y. Chin, F.H. Suhaimi, A. Fairus, S. Ima-Nirwana, Animal models of metabolic syndrome: a review, Nutr. Metab. 13 (2016) 65, https://doi.org/10.1186/s12986-016-0123-9.
[39] Wayhart, J. P., Lawson, H. 2017. Sayfa 1198. Animal models of metabolic syndrome. In Animal Models for the Study of Human Disease. Editör: Conn, P.M. Washington: Elsevier Inc.
[40] J. Wood, M. Tse, X. Yang, D. Brobst, Z. Liu, B. Pang, W.S. Chan, A.M. Zaw, B. Chow, K. Ye, C.W. Lee, C.B. Chan, BDNF mimetic alleviates body weight gain in obese mice by enhancing mitochondrial biogenesis in skeletal muscle, Metab. Clin. Exp. 87 (2018) 113–122, https://doi.org/10.1016/j.metabol.2018.06.007.
[41] A. Ajoolabady, S. Liu, D.J. Klionsky, G. Lip, J. Tuomilehto, S. Kavalakatt, D. M. Pereira, A. Samali, J. Ren, ER stress in obesity pathogenesis and management, Trends Pharmacol. Sci. 43 (2) (2022) 97–109, https://doi.org/10.1016/j.tips.2021.11.011.
[42] J. Yong, J.D. Johnson, P. Arvan, J. Han, R.J. Kaufman, Therapeutic opportunities for pancreatic β-cell ER stress in diabetes mellitus. Nature reviews, Endocrinology 17 (8) (2021) 455–467, https://doi.org/10.1038/s41574-021-00510-4.
[43] S.H. Back, R.J. Kaufman, Endoplasmic reticulum stress and type 2 diabetes, Annu. Rev. Biochem. 81 (2012) 767–793, https://doi.org/10.1146/annurev-biochem-072909-095555.
[44] J. Yong, V.S. Parekh, S.M. Reilly, J. Nayak, Z. Chen, C. Lebeaupin, I. Jang, J. Zhang, T.P. Prakash, H. Sun, S. Murray, S. Guo, J.E. Ayala, L.S. Satin, A. R. Saltiel, R.J. Kaufman, Chop/Ddit3 depletion in β cells alleviates ER stress and corrects hepatic steatosis in mice, Sci. Transl. Med. 13 (604) (2021), eaba9796, https://doi.org/10.1126/scitranslmed.aba9796.
[45] B. Song, D. Scheuner, D. Ron, S. Pennathur, R.J. Kaufman, Chop deletion reduces oxidative stress, improves beta cell function, and promotes cell survival in multiple mouse models of diabetes, J. Clin. Invest. 118 (10) (2008) 3378–3389, https://doi.org/10.1172/JCI34587.
[46] B.B. Boland, C.J. Rhodes, J.S. Grimsby, The dynamic plasticity of insulin production in β-cells, Mol. Metab. 6 (9) (2017) 958–973, https://doi.org/10.1016/j.molmet.2017.04.010.
[47] J. Chen, K.W. Chua, C.C. Chua, H. Yu, A. Pei, B.H. Chua, R.C. Hamdy, X. Xu, C. F. Liu, Antioxidant activity of 7,8-dihydroxyflavone provides neuroprotection against glutamate-induced toxicity, Neurosci. Lett. 499 (3) (2011) 181–185, https://doi.org/10.1016/j.neulet.2011.05.054.
[48] R. Zhang, K.A. Kang, M.J. Piao, D.O. Ko, Z.H. Wang, W.Y. Chang, H.J. You, I.K. Lee, B.J. Kim, S.S. Kang, J.W. Hyun, Preventive effect of 7,8-dihydroxyflavone against oxidative stress induced genotoxicity, Biol. Pharm. Bull. 32 (2) (2009) 166–171, https://doi.org/10.1248/bpb.32.166.
[49] S.A. Villalta, J. Lang, S. Kubeck, B. Kabre, G.L. Szot, B. Calderon, C. Wasserfall, M. A. Atkinson, R.A. Brekken, N. Pullen, R.H. Arch, J.A. Bluestone, Inhibition of VEGFR-2 reverses type 1 diabetes in NOD mice by abrogating insulitis and restoring islet function, Diabetes 62 (8) (2013) 2870–2878, https://doi.org/10.2337/db12-1619.
[50] N. Chitranshi, V. Gupta, S. Kumar, S.L. Graham, Exploring the molecular interactions of 7,8-dihydroxyflavone and its derivatives with TrkB and VEGFR2 proteins, Int. J. Mol. Sci. 16 (9) (2015) 21087–21108, https://doi.org/10.3390/ijms160921087.
[51] R.W. O'Rourke, Inflammation in obesity-related diseases, Surgery 145 (3) (2009) 255–259, https://doi.org/10.1016/j.surg.2008.08.038.
[52] T. Thoudam, J.H. Jeon, C.M. Ha, I.K. Lee, Role of mitochondria-associated endoplasmic reticulum membrane in inflammation-mediated metabolic diseases, Mediat. Inflamm. 2016 (2016) 1851420, https://doi.org/10.1155/2016/1851420.
[53] J. Hirosumi, G. Tuncman, L. Chang, C.Z. Görgün, K.T. Uysal, K. Maeda, M. Karin, G.S. Hotamisligil, A central role for JNK in obesity and insulin resistance, Nature 420 (6913) (2002) 333–336, https://doi.org/10.1038/nature01137.
[54] B.S. Zha, H. Zhou, ER stress and lipid metabolism in adipocytes, Biochem. Res. Int. 2012 (2012) 312943, https://doi.org/10.1155/2012/312943.
[55] E.A. Vilas-Boas, D.C. Almeida, L.P. Roma, F. Ortis, A.R. Carpinelli, Lipotoxicity and β-cell failure in type 2 diabetes: oxidative stress linked to NADPH oxidase and ER stress, Cells 10 (12) (2021) 3328, https://doi.org/10.3390/cells10123328.
[56] N.M. Templeman, S. Skovsø, M.M. Page, G.E. Lim, J.D. Johnson, A causal role for hyperinsulinemia in obesity, J. Endocrinol. 232 (3) (2017) R173–R183, https://doi.org/10.1530/JOE-16-0449.
[57] S. Wang, R.J. Kaufman, The impact of the unfolded protein response on human disease, J. Cell Biol. 197 (7) (2012) 857–867, https://doi.org/10.1083/jcb.201110131.
[58] S. Bhuvaneswari, B. Yogalakshmi, S. Sreeja, C.V. Anuradha, Astaxanthin reduces hepatic endoplasmic reticulum stress and nuclear factor-κB-mediated inflammation in high fructose and high fat diet-fed mice, Cell Stress Chaperones 19 (2) (2014) 183–191, https://doi.org/10.1007/s12192-013-0443-x.
[59] J. Yung, A. Giacca, Role of c-Jun N-terminal kinase (JNK) in obesity and type 2 diabetes, Cells 9 (3) (2020) 706, https://doi.org/10.3390/cells9030706.
[60] D.T. Rutkowski, Liver function and dysfunction - a unique window into the physiological reach of ER stress and the unfolded protein response, FEBS J. 286 (2) (2019) 356–378, https://doi.org/10.1111/febs.14389.
[61] W. Jin, Regulation of BDNF-TrkB signaling and potential therapeutic strategies for Parkinson's disease, J. Clin. Med. 9 (1) (2020) 257, https://doi.org/10.3390/jcm9010257.
[62] L. Wei, L.Y. Kan, H.Y. Zeng, Y.Y. Tang, H.L. Huang, M. Xie, W. Zou, C.Y. Wang, P. Zhang, X.Q. Tang, BDNF/TrkB pathway mediates the antidepressant-like role of H2S in CUMS-exposed rats by inhibition of hippocampal ER stress, NeuroMolecular Med. 20 (2) (2018) 252–261, https://doi.org/10.1007/s12017-018-8489-7.
[63] S. Cırrık, G. Hacioglu, S.N. Ayyıldız, B. Tezcan, İ. Abidin, S. Aydın-Abidin, T. Noyan, Renal response to tunicamycin-induced endoplasmic reticulum stress in BDNF heterozygous mice, Adv. Clin. Exp. Med. 28 (9) (2019) 1161–1170, https://doi.org/10.17219/acem/100647.
[64] S. Cırrık, G. Hacioglu, İ. Abidin, S. Aydın-Abidin, T. Noyan, Endoplasmic reticulum stress in the livers of BDNF heterozygous knockout mice, Arch. Physiol. Biochem. 125 (4) (2019) 378–386, https://doi.org/10.1080/13813455.2018.1489850.
[65] M. Berenguer, J. Zhang, M.C. Bruce, L. Martinez, T. Gonzalez, A.A. Gurtovenko, T. Xu, Y. Le Marchand-Brustel, R. Govers, Dimethyl sulfoxide enhances GLUT4 translocation through a reduction in GLUT4 endocytosis in insulin-stimulated 3T3-L1 adipocytes, Biochimie 93 (4) (2011) 697–709, https://doi.org/10.1016/j.biochi.2010.12.013.
[66] H. Wang, R.E. Scott, Inhibition of distinct steps in the adipocyte differentiation pathway in 3T3 T mesenchymal stem cells by dimethyl sulphoxide (DMSO), Cell Prolif. 26 (1) (1993) 55–66, https://doi.org/10.1111/j.1365-2184.1993.tb00006.x.